Faraday Discussions

RSC Publishing

Cite this: *Faraday Discuss.*, 2013, **166**, 361

PAPER

View Article Online
View Journal | View Issue

A structural study of the self-assembly of a palmitoyl peptide amphiphile

M. Nieuwland, L. Ruizendaal, A. Brinkmann, L. Kroon-Batenburg, J. C. M. van Hest and D. W. P. M. Löwik*

Received 19th April 2013, Accepted 28th May 2013
DOI: 10.1039/c3fd00055a

Peptide amphiphiles consisting of a hydrophobic alkyl tail coupled to the eight-amino acid GANPNAAG have been studied extensively for their fibre forming properties. However, detailed characteristics of the fibre structure, such as peptide conformation and molecular organisation, are unknown to date. In this report a range of characterization techniques is described that have been employed to elucidate the internal structure of these fibres. Based on the results obtained by circular dichroism spectroscopy, X-ray diffraction and solid state NMR spectroscopy it was concluded that in a self-assembled state the peptide is in a stretched β-sheet conformation, with the alkyl tails interdigitated and hydrogen-bonded along the axis of the fibre.

Introduction

Peptide amphiphiles are a versatile class of building blocks with interesting self-assembly characteristics[1–5] In our group, a specific type of peptide amphiphile has been developed by connecting the short, eight-amino acid peptide with the sequence GlyAlaAsnProAsnAlaAlaGly (GANPNAAG), derived from the CS protein of the malaria parasite *Plasmodium Falciparum*,[6] to a series of hydrophobic tails.[7–9] The assembly behaviour of these peptide amphiphiles as a function of tail length has been studied in great detail.[10] It was demonstrated that amphiphiles with a short tail (<12 carbon atoms) did not aggregate, and that the peptide part was in a random coil conformation. It is assumed the hydrophobic driving force is not large enough to induce assembly. With a long tail (>18 carbon atoms) the strong hydrophobic interactions caused the formation of random aggregates. For alkyl chains between 12 and 18 carbons long the driving force of the hydrophobic tail was large enough to induce assembly, which was also directed by the hydrogen bonds between the amino acids that contributed to the assembly process. Because of these directional hydrogen bonds, the amphiphiles packed into fibres which were stable at room temperature and disassembled reversibly upon heating. However, even though we know how to make and manipulate the fibres,[11–14] the

Radboud University Nijmegen, Institute for Molecules and Materials, Department of Bio-Organic Chemistry, Heyendaalseweg 135, 6525 AJ Nijmegen, The Netherlands. E-mail: d.lowik@science.ru.nl

organisation of the peptide amphiphiles in the fibres and what kind of conformation the peptide fragment possessed after fibre assembly remained elusive to date. In order to be able to design *de novo* these kinds of self-assembled architectures, the molecular assembly and the influence of small changes in the building blocks on the final assembly have to be fully understood. In this paper we describe our detailed investigations to elucidate the molecular structure of fibres derived from the GANPNAAG peptide N-terminally coupled to a 16 carbon atom palmitoyl tail (PA **1**, Fig. 1a).

Possible models for peptide amphiphile packing

In order to obtain more insight into the structure of the peptide amphiphile fibres, first the different possibilities for packing of the peptide amphiphiles, with respect to alkyl chains and peptide head group, were defined. For the alkyl part of the amphiphile two possible packings were considered, one in which the tails at one side of the bilayer do not overlap with the other side, and one in which the tails interdigitate completely (Fig. 1b). Other packings were considered to be unlikely, because they often involve unfavourable voids within the fibrous structure. For the peptide some more conformational possibilities were taken into account. It contains a proline, which, due to its restricted

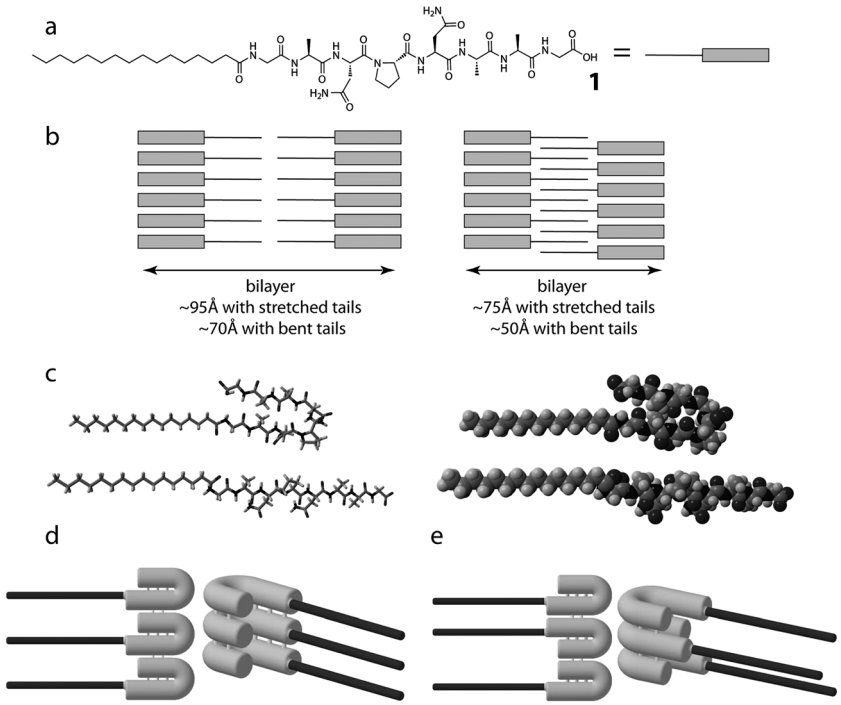

Fig. 1 Important considerations with respect to fibre formation. a) Structure and schematic representation of PA **1**. b) The two possible arrangements for the alkyl tail. c) Two extreme peptide conformations, shown both as a Dreiding and a CPK model. d) The hydrogen bond direction for the peptides in a turn, which can be either within (left) or perpendicular to the plane of the turn (right). The peptide amphiphiles with a turn may be d) symmetrically or e) asymmetrically stacked.

backbone conformation, is in general associated with turns in a protein. Furthermore, the active conformation of the peptide NPNA, the repeating unit in the CS protein of the malaria parasite *Plasmodium Falciparum* and the basis of the peptide we employ, has been shown to favour an anti-parallel β-hairpin.[15] Hydrogen bonds stabilise the turn, and the side chains are oriented perpendicular to the plane of the turn. Although the peptide GANPNAAG is based on the NPNA motif, the hydrophobic tail introduces additional interactions and therefore the peptide could possibly fold differently from the β-turn observed in NPNA crystals.[15] Therefore other conformations up to the extreme of a stretched peptide were considered (Fig. 1c). A third important parameter of the fibre packing is the directionality of the hydrogen bonds. They may be present along the long or short axis of the fibre causing the amphiphile–amphiphile distance in that direction to be ~4.5 Å. The side chains perpendicular to the hydrogen bonds will give rise to distances between the molecules of at least 6 Å. A similar kind of variation in orientation can be found, in case of a turn conformation, for the plane of the turn, in the length or width of the fibre. Furthermore, the hydrogen bonds may be in the plane of the turn, as for the crystals of NPNA,[15] or perpendicular to the turn (Fig. 1d). In the latter case, turn formation is driven by hydrophobic interactions, and side chains of the amino acids are present in the turn. Finally peptide amphiphiles that adopt a turn-conformation may pack symmetrically or asymmetrically in the fibre, yielding more possibilities to assemble for the folded than for the straight peptide. In Fig. 1e one of the possible asymmetric packings for both hydrogen bond directions is given.

Based on these conformational parameters 12 possible models were considered (A–L), which are summarized in Table 1. In a first approximation the symmetry of the packing of the turn conformation peptides has not been considered in these models.

To determine the morphology of the assemblies and to obtain information on the width and height of the fibres, a variety of microscopy techniques were employed: transmission electron microscopy (TEM) and atomic force microscopy (AFM) were performed on dried samples, and cryo-TEM on fibres in quickly-frozen solution, to elucidate the morphology in solution avoiding artefacts of the

Table 1 A summary of the structural features of each of the considered models for molecular packing

Model	Peptide	H-bond direction		Alkyl tails
A	Straight	Along fibre length		Overlapping
B				Non-overlapping
C		Along fibre width		Overlapping
D				Non-overlapping
E	In a turn	Along fibre length	Within the turn	Overlapping
F				Non-overlapping
G			Perpendicular to turn	Overlapping
H				Non-overlapping
I		Along fibre width	Within the turn	Overlapping
J				Non-overlapping
K			Perpendicular to turn	Overlapping
L				Non-overlapping

drying-in effects. The secondary structure of the peptide was investigated using circular dichroism (CD) spectroscopy, with which the most important secondary structures in proteins – the α-helix, β-sheet and random coil – can be distinguished. Furthermore, close contacts between nuclei in dried fibres were determined using solid state NMR (ssNMR) on amphiphiles labelled with ^{13}C and ^{15}N NMR active nuclei. Finally, to determine spacings within the fibre, X-ray diffraction was used, both on dried-in samples and fibres in solution in conjunction with nuclear magnetic resonance (NMR).

Microscopy

Dried samples

Transmission electron microscopy (TEM) revealed micrometer long, twisted ribbons with a width of about 25 nm (Fig. 2). The same architectures were observed with atomic force microscopy (AFM) (Fig. 3) on glass and fused silica. The fibres were observed both in height and in phase mode, showing the presence of assemblies (height mode) and also the difference of material properties between the assemblies and the underlying substrate (phase mode). Typically, in the AFM pictures with mica as a substrate, assemblies of two different heights were visible (most clearly visible in the centre picture of Fig. 3). This may be due to a drying effect, or an interaction with the mica. Because of the presence of similar fibres on a range of substrates, we concluded that the presence of the fibrous structures was not due to substrate effects.

Solution samples

The fibre formation in solution was confirmed using cryo-TEM measurements. The PAs were again found to be assembled into twisted ribbons, with a width of approximately 25 nm (Fig. 4) and an irregular twist. The relatively large distribution in width of the fibres that was observed, shown in Fig. 4b, is probably caused by the low contrast in the cryo-TEM measurements, due to the absence of any staining or shadowing step in the preparation of the samples.

The morphology of the fibres depends on the molecular packing of the fibres, but it cannot be directly correlated to the packing as shown in Fig. 1 from these microscopy pictures. The observed twisted ribbon structure is indicative of fibres which consist of stacks with a width of 25 nm which extend in length up to micrometers. Unfortunately, the thickness of the bilayer is too small to be measured reliably with electron microscopy.

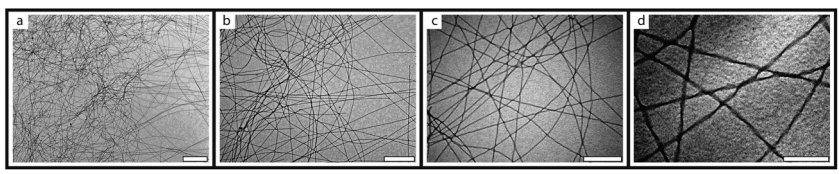

Fig. 2 TEM graphs of PA **1**. The succeeding images show a zoom of the same spot. The white bars represent a) 2 μm, b) 1 μm, c) 500 nm, d) 200 nm.

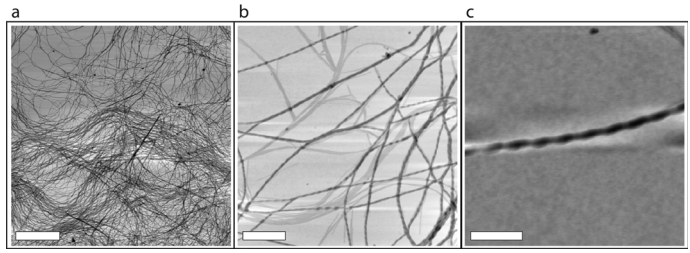

Fig. 3 AFM height pictures of PA **1** on mica. The white bars represent a) 4 μm, b) 500 nm, c) 200 nm.

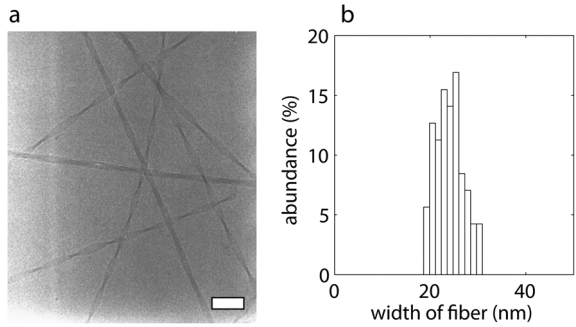

Fig. 4 a) Cryo-TEM picture of PA **1**. The white bar represents 100 nm. b) Width distribution of the fibres.

Circular dichroism (CD)

The conformation of the peptide moieties was probed using CD spectroscopy. As observed earlier for any GANPNAAG peptide which was modified with an alkyl tail of 14 carbons or longer, PA **1** yielded an enhanced β-sheet-like signal (Fig. 5b). As a comparison, coupling of a short (or no) tail to the GANPNAAG peptide resulted in a random coil signal in the CD spectrum (Fig. 5a).[16] The signal at 196 nm is higher than expected for a standard β-sheet signal, because of an interfering linear dichroism (LD) effect, which is caused by a macroscopic orientation of the fibres in the solution resulting in an additional contribution to the CD signal.[17]

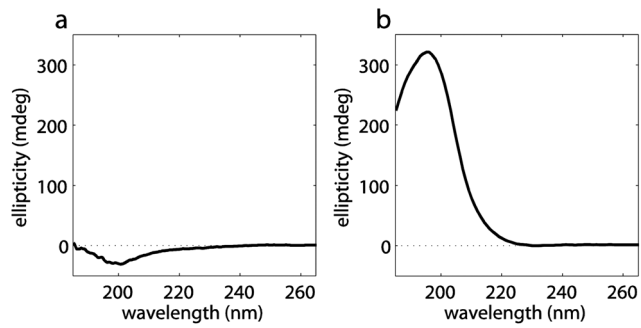

Fig. 5 CD spectra of a) GANPNAAG coupled to lauric acid (C_{12})[16] and b) PA **1**.

H–D exchange measurements

By determining the ease with which protons exchange with solvent it is possible to identify amino acids positioned at the periphery of a protein or peptide assembly.[18–20] In particular amide protons are amenable to such exchange in a protic solvent. The more solvent-exposed the amide protons are, the faster this exchange is. If a protein is prepared in water, it can be diluted into D_2O and an exchange of protons for deuterons will take place. For the fibres, measuring the exchange rate could elucidate if the peptides are stretched or in a turn conformation. Unfortunately, employing both ^{1}H NMR and mass spectrometry to detect the H–D exchange, no conclusive results were obtained that might be assigned to a specific molecular architecture.

Solid state nuclear magnetic resonance spectroscopy (ssNMR)

To determine the packing of the amphiphiles and elucidate the local structure of the molecules first NMR spectroscopy was employed.[21–23] In particular solid state NMR (ssNMR) on lyophilised samples was used. In ssNMR, the samples are spun very fast around a so-called magic angle (MAS, magic angle spinning) averaging anisotropic interactions to increase resolution. In addition, the presence of protons (^{1}H) shields neighbour atoms such as carbons (^{13}C) and nitrogens (^{15}N) *via* dipole–dipole interactions, leading to line broadening too. To eliminate this effect, a high radio frequency (RF) ^{1}H decoupling was used. Under such conditions, spectral resolution in ssNMR is increased and high-resolution measurements can be performed. One way to elucidate the amphiphile packing in the fibre is by measuring distances between labelled positions in the molecule. The technique we employed in this study was rotational echo double resonance (REDOR).[23] With this method magnetisation is transferred from ^{1}H to, in this case, ^{15}N (see Fig. 6 for the pulse sequence). The magnetisation on nitrogen is dephased for a period τ, and rephased after a π pulse for the same period. After that, the ^{15}N spectrum is recorded. During the period τ, π pulses are applied on ^{13}C which cause dipole–dipole interaction effects on the ^{15}N spectrum only if the ^{13}C and ^{15}N are close enough. The difference between the spectra with and

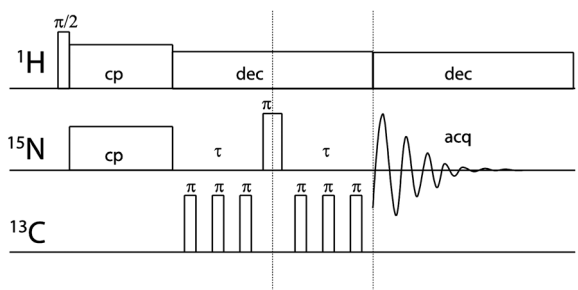

Fig. 6 Pulse sequence for a REDOR experiment. The number of π pulses on the ^{13}C channel depends on the length of τ and the sample spinning speed. cp denotes crosspolarisation, dec decoupling and acq acquisition.

without pulses on ^{13}C is dependent on the inverse cube of the distance between the nitrogen and carbon atoms. Therefore, this technique measures distances reliably up to about 5 Å. To employ REDOR, we prepared amphiphiles labelled with NMR-active nuclei. ^{13}C and ^{15}N were incorporated at the methyl group of the C_{16} tail (**I**), the nitrogen of the first glycine (**II**) and the carbonyl carbon of the last glycine (**III**, see Fig. 7). When the peptide is folded into a perfect hairpin structure, in which hydrogen bridges are present within the molecule (models E–F and I–J), the distance between nuclei **II** and **III** is 3Å, close enough to determine using ^{15}N-^{13}C-REDOR NMR. Intermolecular close contacts between **I** nuclei could disclose whether the alkyl tails of the two bilayers were overlapping or not, while possible interactions between **I** and **II** or **I** and **III** might reveal to what extent the alkyl tails were overlapping.

Carbon spectra of naturally abundant PA fibres were acquired to determine the effect of several rehydration times, one of the parameters investigated for amyloid fibres for which the exact fibre structure is extremely sensitive in the fibre preparation.[22] These spectra were recorded in a cross-polarisation experiment, in which magnetisation is transferred from protons to carbons and the carbon spectrum was measured. At first sight, the spectra were similar, but since the spectra had a poor signal-to-noise ratio small structural differences between the samples may not have been resolved.

After these experiments on the naturally abundant PAs, single-pulse ^{15}N spectra of the labelled amphiphiles were acquired. These spectra showed several ^{15}N resonances, whereas only one was expected since PA **1** possessed only one ^{15}N label. This suggested that more than one chemical environment was present for the ^{15}N atoms, which was surprising, since this was not observed in the ^{13}C spectra. However, since the carbon spectra had a poor signal-to-noise ratio differences among the samples may not have been resolved, as mentioned above. A cause of the difference in the environment of the ^{15}N nuclei could be damage of the fibres due to freezing.[9] Furthermore, the fibres can be considered to exist in a kinetically-trapped state, and thus a collection of architectures may be present. Another reason for the observed variety of environments could be the presence of unstructured aggregates in the solution before lyophilisation. To validate this assumption a sample was prepared in which the final annealing step (heating to 90 °C and slow cooling) was omitted, which should result in more disordered fibres and consequently yield more and broader peaks. On the other hand, a sample with an expected better defined fibre conformation was prepared by centrifugation of the sample, after which the supernatant was removed prior to lyophilisation. The removal of the liquid should remove dissolved amphiphiles, yielding a sample containing only fibres. Of course, it does not exclude the presence of large

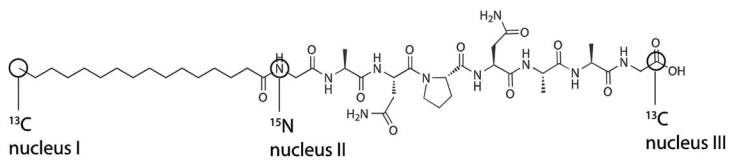

Fig. 7 ^{13}C and ^{15}N isotopically labelled PA **1** employed in the ssNMR REDOR experiment.

random aggregates that would still hamper the measurements. Surprisingly, the ultra-centrifuged sample showed broader peaks than the sample in which the annealing step was omitted, while the opposite result was expected. Besides the broadness of the peaks, no additional spectral differences between these samples and the original one were observed. Therefore a variety of environments was also present for the ^{15}N atoms with these preparation methods.

To examine whether the homogeneity of the fibres is affected by the pH at which they are prepared, the PA was dispersed in volatile buffers of three different pHs (4, 7 and 10) and lyophilised. At pH 4, more peaks were observed than under alkaline conditions, indicating a less defined fibre (Fig. 8). This was confirmed using TEM measurements and can be explained from the molecular structure of the PAs. Under acidic conditions, the free carboxylic acid ends of the peptides are protonated and the repulsive forces are reduced. Therefore, the tendency for peptide aggregation will be stronger and the assembly faster, resulting in less ordered fibres. Moreover, with decreased repulsive forces, heating to 90 °C might not be enough to disassemble the fibres, thus also yielding less ordered aggregates. However, a single peak was not observed either for the samples prepared in alkaline conditions, nor for those prepared at low pH – neither preparation method resulted in a single environment for the ^{15}N atoms.

Despite the fact that none of the conditions that were tried resulted in a single peak ^{15}N spectrum, a REDOR experiment was carried out to determine the distance between nuclei **II** and **III** within one amphiphile. To prevent intermolecular interactions from interfering, we used a 1 : 9 ratio of labelled amphiphile to natural abundance PA. Under these circumstances, only intramolecular interactions are expected to be visible. In the experiment, the signal intensity of

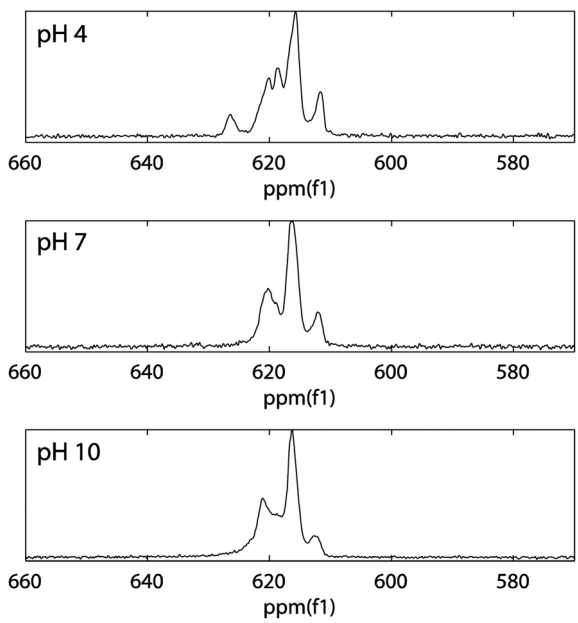

Fig. 8 Nitrogen spectra of labelled C_{16}-GANPNAAG-OH, prepared at three pH values.

an experiment with pulses on carbon was compared to an experiment where these π pulses were omitted, as explained above. The two obtained signals did not differ significantly, indicating that the two nuclei are far apart. Due to a small signal-to-noise ratio distances larger than 4.7 Å could not be determined, and therefore it could only be concluded that the distance between nuclei **II** and **III** was larger than 4.7 Å, and thus that the peptides could not be in a perfect β-turn conformation, in which the hydrogen bonds are present within the turn.

X-ray diffraction

To determine molecular order in the fibres in more detail we turned to X-ray diffraction. Generally, soft samples or samples in solution are more difficult to measure than crystalline samples, since these samples are less ordered. Nevertheless, soft samples such as fibres can still give X-ray diffraction patterns because in these structures the distances of the molecules within fibre are highly repetitive. When bundles of fibres are present, even the width of a single fibre can be distinguished. Both dried-in samples and fibres in solution were measured using several set-ups. Since the fibres assemble in solution and may change structure due to external influences – like temperature and pH – we were primarily interested in the architecture of the fibre in solution. Changes in structure as a result of external influences would then be easy to measure as well. However, measuring solid samples was also of interest since first a much higher concentration of PAs could be obtained, providing a better signal-to-noise ratio, and secondly a possible structural change upon drying of the samples could be investigated.

Small angle X-ray scattering (SAXS)

To investigate 'large' (between 10 and 5000 Å) features of the fibres, such as the bilayer width, small angle X-ray scattering was used.[24,25] As can be seen in Fig. 1, a stretched peptide results in a fibre width of approximately 75 Å with intercalating alkyl tails and about 95 Å when the tails do not overlap. A peptide oriented in a perfect β-hairpin yields a bilayer width of circa 50 Å for intercalating and 70 Å for non-overlapping tails. In solution the largest observed diffraction peak corresponded with 54 Å (Table 2), suggesting intercalating tails and peptides in a turn conformation (models E, G, J and L, Table 1). At these small angles, however, not only repetitive distances but also the so-called form-factor play an important role in the appearance of the diffraction pattern. No higher order reflections are discernible, indicating that indeed the form-factor may be the cause of this peak. Furthermore, the 54 Å signal is very broad, and may therefore just depict the size of one (non-repetitive) bilayer. After drying, a much sharper peak at 73 Å was observed instead (Fig. 9a), suggesting either a bent peptide with non-overlapping tails or a straight peptide with overlapping tails (models A, C, F, H, J and L). The difference in observed fibre width between solution and dried samples (54 Å and 73 Å respectively) can be accounted for by assuming a lower degree of order of solvent-exposed amino acids in the solution samples. Therefore, the very broad 54 Å signal, associated with the bilayer, may only have shown the central part of the bilayer because the rest was too flexible. On drying, the fibres get closer together and pack with several bilayers on top of each other. In this situation, all

Table 2 Measured spacings with several X-ray techniques. Dark grey means the distance could not be observed in that particular set-up, while light grey are data which were obtained very close to the beam stop and are therefore less reliable. The last column shows the interpretation of the peaks using model A

q	D (Å)	SAXS (solution)	SAXS (dried-in)	Capillary (solution)	Capillary (dried-in)	Reflection (dried-in)	Possible plane (model A)
1.65	3.8			x	x	x	combination (100 and 010)
1.40	4.5				x		hydrogen bridge (100)
1.35	4.7			x	x		hydrogen bridge (100)
1.02	6.2				x	x	
0.84	7.5				x	x	perpendicular to β-sheet
0.61	10.3				x		perpendicular to peptide (010)
0.43	14.6	x	x		x	x	bilayer thickness (005)
0.34	18.5	x	x		x	x	bilayer thickness (004)
0.17	36.5		x			x	bilayer thickness (002)
0.12	54.2	x		x			non-ordered bilayer (001)
0.095	66.1				x		slightly ordered bilayer (001)
0.088	71.4					x	bilayer thickness (001)
0.086	73.0		x				bilayer thickness (001)

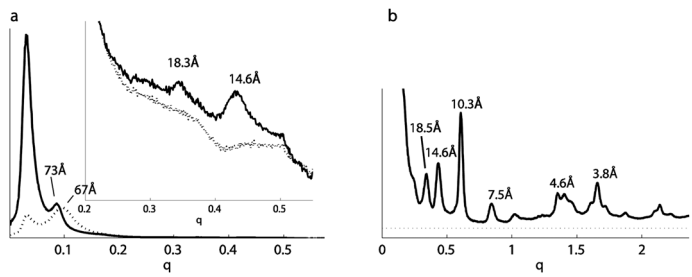

Fig. 9 Two examples of X-ray diffraction patterns of PA **1**. a) SAXS measured using synchrotron radiation on dried-in samples from water (solid line) and acetic acid (dotted line). The inset shows an enlargement of these diffraction patterns. b) Capillary mode measurement measured using Cu Kα radiation of a dried-in sample.

residues of the peptide are locked in a defined conformation, and the 'real' bilayer thickness can be observed. Amphiphiles freeze-dried from acetic acid were anticipated to be a control with respect to the dried samples, since we assumed that no aggregation would take place in this solvent. Unexpectedly, this solid sample also showed a peak in the X-ray measurements corresponding to a distance of 67 Å. Nevertheless, the observed peak was very broad, merely depicting a repeating distance in an un-ordered system. In solution and in dried samples, but not in the PAs lyophilised from acetic acid, peaks were also observed at 18.5 Å and 14.6 Å. We expect these to be higher order peaks of the bilayer distance (see General discussion section).

Capillary mode measurements

Smaller features of the peptides were investigated in solution, measured in a capillary which was placed in a position perpendicular to a weaker Cu Kα X-ray beam. In contrast to the SAXS measurements, the wavelength could not be tuned and much longer measurement times were needed. Upon filling the capillary, the flow induced partial alignment of the fibres. Because this orientation was along the length of the capillary, perpendicular to the beam, as a result distances along the fibres could be determined. Furthermore, because of the preferred orientation, the sample did not resemble a completely randomly oriented powder. Therefore the orientation of some interplanar spacings relative to each other could be determined. For example, it was determined that the measured 4.7 Å, 4.5 Å and 4.3 Å distances were oriented perpendicular to the 7.5 Å, 10.3 Å, 14.6 Å and 18.5 Å spacings (see below). After drying of the solution within the capillary, the sample was measured again, yielding a better-resolved diffractogram (Fig. 9b). The preferred orientation of the fibres in the capillary was lost upon drying. However, no structural change was induced and the circularly integrated diffractogram showed the same peak positions as the solution sample. Conservation of the structure upon drying was also suggested by the microscopy techniques. An overview of observed peaks is given in Table 2. The peaks at 4.7 Å, 4.5 Å and 4.3 Å support the packing of the peptides into a β-sheet conformation, and should be visible both for the linear and turn conformations. Also the 3.8 Å peak is commonly observed in this type of cross β-sheet structures. The 7.5 Å, 10.3 Å, 14.6 Å and 18.5 Å peaks are associated with spacings perpendicularly oriented to the β-sheet, that can either be assigned to bilayer dimensions or packing of the peptides in the non-hydrogen bonded direction of the β-sheet.

Reflection mode experiments

Samples dried on a silicon plate were measured in reflection mode. In this orientation, the measurements did not resolve typical β-sheet distances. TEM and AFM on several substrates showed that the fibres were lying with their long axis parallel to the surface, which is therefore the expected orientation on silicon as well. With the long axis parallel to the surface, the repetitive planes within that axis do not cause reflection and are therefore not detected. The absence of β-sheet signals suggests that the β-sheet direction is along the length of the fibre, thus supporting models A, B and E–H. The peaks that were detected were in line with the other X-ray experiments (Table 2).

A summary of the results of all X-ray measurements is given in Table 2. In our opinion from these results a possible unit cell can be proposed of $73.5 \times 10.3 \times 4.7$ Å^3, which leads us to a proposed model with a stretched peptide and interdigitating tails perpendicular to the long fibre axis (models A and C) or a model with the peptide in a turn and tails which were not overlapping (models F, H, J or L). A more elaborate explanation of the results is given in the general discussion.

General discussion

From electron microscopy and AFM, we conclude that the eight-amino acid peptide GANPNAAG assembles into fibrous architectures in aqueous solution

when coupled to an alkyl tail of 16 carbon atoms. The observed twisted ribbons had a width of about 25 nm (determined with cryo-TEM) and were tens to hundreds of micrometers long (as observed with TEM, AFM and cryo-TEM).

The possible models for the molecular packing are summarized in Fig. 1, and result from differences in the overlap of the alkyl tails, conformation of the peptide (stretched or in a β-hairpin) and direction of the hydrogen bond (width or length of fibre). If the peptides adopt a β-hairpin conformation, some more possibilities could be considered. The hydrogen bonds may localise in the turn or form perpendicular to the turn, and the peptides may stack symmetrically or asymmetrically in the fibre. In Table 3 the reasons to reject models are summarized. CD spectroscopy measurements confirmed the validity of a model in which the peptides are oriented in a β-sheet fashion (as in all of the models A–L).

The diffraction experiments showed a β-sheet packing, which agreed with the CD experiments, but the diffraction data also contained more information. In the reflection mode experiments the typical β-sheet spacings of 4.3, 4.5 and 4.7 Å were not observed, while they were present in the capillary mode experiments. Distances parallel to the surface are not observable in the reflection mode experiments, and therefore the β-sheet direction should be parallel to the surface. In the TEM and AFM the fibres were shown to lie flat on several substrates, which is therefore also the expected orientation on silicon, the substrate for X-ray reflection experiments. The flat orientation of the fibres combined with the β-sheet signal not being observed suggests that the β-sheet direction is along the

Table 3 Summary of reasons for which the different models are discarded. 'No β-sheet observed' refers to the absence of typical β-sheet spacings in reflection mode X-ray experiments. The entries labelled 'Bilayer' are discarded because of the incompatibility of the bilayer width in that model with the observed 73 Å. For those labelled 'ssNMR' the ssNMR measurements showed that the peptides are not in a perfect fold and the entries 'Empty space' are less likely because of thermodynamic considerations

Model	Peptide	H-bond direction		Alkyl tails	Discarded because			
A	Straight	Length		Overlapping				
B				Non-overlapping		Bilayer		
C		Width		Overlapping	No β-sheet observed			
D				Non-overlapping	No β-sheet observed	Bilayer		
E	In a turn	Length	In turn	Overlapping		Bilayer	ssNMR	
F				Non-overlapping			ssNMR	Empty space
G			Perpendicular	Overlapping		Bilayer		
H				Non-overlapping				Empty space
I		Width	In turn	Overlapping	No β-sheet observed	Bilayer	ssNMR	
J				Non-overlapping	No β-sheet observed		ssNMR	Empty space
K			Perpendicular	Overlapping	No β-sheet observed	Bilayer		
L				Non-overlapping	No β-sheet observed			Empty space

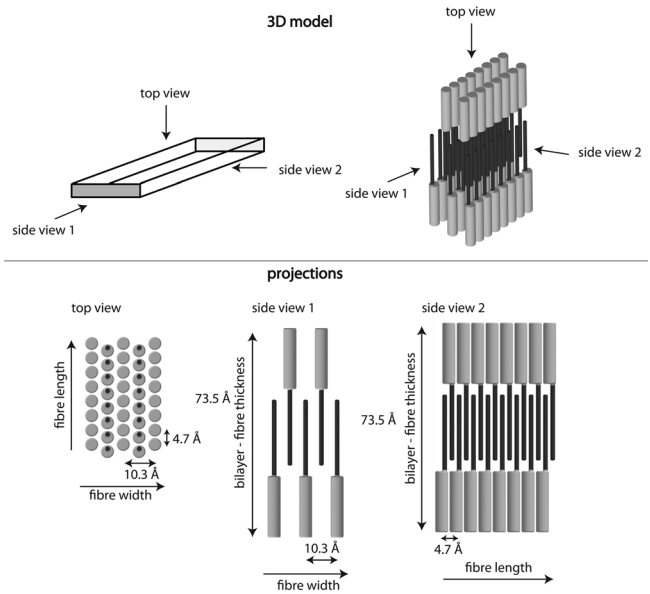

Fig. 10 The model of the PA fibre which combines the observations from all performed measurements.

long axis of the fibre. This was confirmed by polymerisation experiments on similar PAs with a diacetylene moiety in the hydrophobic tail.[8,12,13] Diacetylenes can only polymerise if the distance between adjoining units is approximately 4.5 Å, a distance which coincides with the hydrogen bond direction. Since we observed the polymerisation to take place in the long axis direction of the fibre, this should be the hydrogen bond direction. Therefore, models C, D and I–L are discarded.

From the X-ray results in solution, the bilayer width seemed to be 54 Å, which could be compatible with a model in which the peptide is in a turn conformation (models E–L) and the alkyl tails intercalate (leaving models E, G, I and L). However, with this unit cell the interpretation of the peaks remains unsatisfactory. Either peaks do not really fit within the model or are missing. Furthermore, the ~73 Å observed in the dried samples cannot be accounted for by this model. Therefore, a unit cell of dimensions $73.5 \times 10.3 \times 4.7$ Å^3 is proposed, which suggests either a bent peptide with non-overlapping tails or a straight peptide with overlapping tails (models A, C, F, H, J and L). The 36.5 Å, 25 Å, 18.5 Å and 14.6 Å peaks were accounted for as higher order peaks of the bilayer (see Table 2). The smaller width of the bilayer in solution (54 Å instead of 73 Å) can be explained by assuming less order of the solvent-exposed amino acids in the solution. Therefore, the very broad 54 Å peak, associated with the bilayer, only reflects the centre part of the bilayer. On drying, the fibres get closer together and pack with several layers of the bilayer upon each other. In this situation, all residues of the peptide are locked in a defined conformation, and the 'real' bilayer thickness is visible. The higher mobility of the peptides in solvent seems more likely for a stretched (A, C) than for a bent peptide (F, H, J), but both are possible. Following this argument, models B, D, E, G, I and K become improbable. From the combined X-ray observations, model A seems the most plausible although H is

also possible. A drawback of this interpretation of the X-ray measurements is the assumed high order in the bilayer direction. For seventh and maybe even tenth order peaks, observed in the dried samples, to show up, the system has to be highly ordered in this direction, while we expected the bilayer direction to be the least ordered.

The solid state NMR measurements excluded the models in which the peptide was folded and the β-sheet was present in a turn (E, F, I and J) which supports the X-ray experiments.

In conclusion, the above-mentioned observations only leave models A and H as possibilities for the amphiphile packing. However, the models in which a turn conformation is combined with non-overlapping tails (models F, H, J and L) would introduce thermodynamically unfavourable empty space into the fibre, and are thus considered less likely models. Furthermore, the increased mobility of the bilayer in solvent may be also easier accounted for by stretched peptides than by peptides in a turn conformation. For both of these reasons, model H is less likely, and therefore we are of the opinion that the fibres are packed according to model A.

Conclusions

A schematic representation of the fibre model that fits all the acquired data (model A) is shown in Fig. 10. PA fibres built up of **1** organise according to this model, which means that the peptides are in a stretched β-sheet conformation, with hydrogen bonds directed along the long axis of the fibre, and with alkyl chains that are interdigitated. These single layer fibres stack *via* both hydrophobic and hydrogen bonding interactions into fibres of 25 nm width and micrometers in length as observed using TEM and AFM.

Experimental section

General

All starting materials were obtained from commercial suppliers and used as received. Thin layer chromatography was performed on Kieselgel F-254 pre-coated silica plates or RP-8 F-254s. Visualization was accomplished using TDM.[26] Column chromatography was carried out on Merck silica gel 60 (230–400 mesh ASTM). ^{1}H NMR spectra were recorded on a Varian Mercury, 400 MHz. DMSO-d_5 ($\delta = 2.50$ ppm) was used as a solvent shift reference. Mass spectra were recorded on a JEOL AccuTOF-CS spectrometer.

Synthesis of the amphiphiles

The GANPNAAG peptide was prepared by standard solid-phase Fmoc protocols.[27] To couple the first glycine to a *p*-alkoxybenzy alcohol resin,[28] the resin was washed three times with dichloromethane and subsequently suspended in dimethylformamide (DMF). Two equivalents of the Fmoc protected glycine, 4 equivalents 1-hydroxybenzotriazole hydrate (HOBt), 2 eq. diisopropylcarbodiimide (DIPCDI) and 2 eq. 4-dimethylaminopyridine (DMAP) were added. The suspension was agitated overnight. The suspension was then filtered, washed and dried under vacuum, to result in a resin with a loading of 0.67 mmol Fmoc-Gly per gram.

In all subsequent couplings we used 3 equivalents of the amino acid, 3.3 equivalents DIPCDI and 3.6 equivalents HOBt in DMF. Deprotections were carried

out using a 20% piperidine solution in DMF. After each coupling and deprotection a Kaiser test[29] was performed to check the completeness of the reactions. After removal of the final Fmoc group the peptide was functionalized on the resin employing 3 equivalents palmitic acid dissolved in dichloromethane to which 3.3 equivalents DIPCDI and 3.6 equivalents HOBT in DMF were added. The product was cleaved from the resin by treatment with trifluoroacetic acid/H_2O/triisopropylsilane (95 : 2.5 : 2.5) for two hours followed by precipitation in ether or removal of the volatiles in vacuo. Column chromatography (eluent: $CHCl_3$/MeOH/H_2O 65 : 25 : 4) and subsequent lyophilization afforded pure compounds according to ^{1}H NMR, MS and TLC.

Yield: 76%, based on Fmoc-Gly loading (0.67 mmol g^{-1}) of initial resin.

TLC: $R_f = 0.33$ (eluent: MeOH/$CHCl_3$/AcOH 25 : 65 : 10).

^{1}H NMR [DMSO-d_6]: $\delta = 0.85$ (t, CH_3 alkyl chain, 3H), 1.12 (d, CH_3 Ala, 3H), 1.20 (m, –CH_2 alkyl chain; CH_3 Ala, 30H), 1.48 (m, CH_2 alkyl chain, 2H), 1.85 (m, CH_2 Pro, 3H), 2.18 (m, CH_2 Pro; α-CH_2 alkyl chain, 3H), 2.40 (m, CH_2 Asn, 2H), 2.55 (dd, CH_2 Asn, 1H), 2.65 (dd, CH_2 Asn, 1H), 3.65 (m, α-CH_2 Gly; CH_2 Pro, 3H), 3.75 (m, CH_2 Pro; α-CH_2 Gly, 3H), 4.20 (m, CH_2 Pro; α-CH_2 Ala, 4H), 4.40 (m, α-CH_2 Asn, 1H), 4.73 (q, α-CH_2 Asn, 1H), 6.92 (s, NH_2 Asn, 1H), 7.10 (s, NH_2 Asn, 1H), 7.20 (s, NH_2 Asn, 1H), 7.52 (d, α-NH Ala, 1H), 7.64 (s, NH_2 Asn, 1H), 7.72 (d, α-NH Ala, 1H), 7.88 (two d, α-NH Asn; α-NH Ala, 2H), 7.96 (broad s, α-NH Gly, 2H), 8.27 (d, α-NH Asn, 1H), 12.45 (broad s, OH, 1H).

Maldi-TOF: Calc. for $[C_{42}H_{72}N_{10}O_{12} + Na]^+$ 931.5, found 931.2.

Fibre preparation

Unless stated otherwise, for preparation of the fibres, the amphiphiles were dispersed in milli-Q water at the desired concentrations. The samples were heated to 50 °C for 30 min, followed by 15 min sonication at that temperature. Subsequently, the samples were heated to 90 °C and allowed to cool to room temperature.

Transmission electron microscopy (TEM)

TEM samples were prepared by floating a carbon-coated copper grid on a peptide amphiphile solution of either 1.0 or 0.2 mg mL^{-1} for 5 min, followed by removal of residual water by blotting with a paper filter. The samples were visualized using a JEOL 1010 transmission electron microscope set on an accelerating voltage of 60 kV.

Cryo-TEM

Samples for the cryo-TEM (PA **1** solution of 5 mg mL^{-1}, prepared following the standard procedure described above) were prepared on carbon-coated copper grids which were treated with ozone to increase their hydrophilicity. A droplet of 3 μl was placed on the grid and excess of sample was blotted with filter paper to leave a thin film on the grid. This film was vitrified in liquid ethane and analyzed in a Philips TEM (CM 12) at −170 °C. The whole sample preparation was carried out in a controlled environment vitrification system to ensure cryofixation of the specimen from a controlled temperature and without loss of water or volatile compounds.

Atomic force microscopy (AFM)

AFM measurements were performed on a DI Dimension 3100. A 5 μL sample of PA **1** with a concentration of 0.2 mg mL^{-1}, prepared following the standard procedure (see above), was placed on either a mica, a glass or a fused silica substrate and allowed to dry. The data were processed using the WSxM software package.[30]

Circular dichroism (CD) spectroscopy

Measurements were carried out at a concentration of 0.2 mg mL^{-1} using a 1 mm quartz cell. The spectra were recorded on a JASCO J-810 spectropolarimeter equipped with a Jasco PTC-423S/L Peltier type temperature control system. Spectra were measured from 265–185 nm at 100 nm min^{-1}. To measure temperature curves, a heating or cooling rate of 3 °C min^{-1} was used. During the heating and cooling the CD intensity was measured at 196 nm.

X-ray diffraction

Small angle X-ray scattering

SAXS experiments were conducted on the SAXS station (BM 26.2) at the Dutch-Flemish beamline (DUBBLE) at the European Synchrotron Radiation Facility in Grenoble, France. During the experiments the ESRF was running at 170 mA, and the monochromator of the SAXS station was set at 1.24 Å. A measuring window from 10 to 200 Å was employed, using a wavelength of 0.95 Å. SAXS data of fibres with a concentration of either 10 or 20 mg mL^{-1} in 2 mm diameter capillaries were recorded with the gas multiwire 2-dimensional detector at a sample to detector distance of 1.5 m. The data were successively normalized for absorption and detector uniformity; the background scattering due to the solvent and empty capillary was subtracted. Spatial calibration was performed with silver behenate,[31] with an estimated error margin of ±0.5 % in the observed periodicities.

Capillary mode

X-ray diffraction data in the capillary mode set-up were recorded on a Mar Image Plate using Cu Kα radiation from a BrukerAXS FR591 generator with a rotating anode and Montel 200 mirrors. A 10 mg mL^{-1} solution of the amphiphile was inserted into a capillary. The samples were measured in the solution state, but were also allowed to dry under ambient conditions. The capillaries were placed in a position perpendicular to the X-ray beam and at a distance of 250 mm from the detector. Scattering of air and the capillary was subtracted by using in-house software (VIEW/EVAL).[32]

Reflection mode

X-ray powder diffraction in reflection mode was performed on dried samples using a Bruker D8 AXS Advance X-ray Diffractometer with a VÅNTEC-1 detector. The diffractometer was equipped with a Johansson type monochromator. The detector was set at an effective angular region of 2°. The data were collected in reflection geometry using monochromatic Cu Kα radiation, 2θ range 0.2–60°, stepsize 0.01° and counting time 10 s.

Solid state nuclear magnetic resonance (ssNMR) spectroscopy

General

For the ssNMR measurements, amphiphiles with three NMR active nuclei were synthesized following standard solid phase chemistry and purification as described for the unlabelled compound. The spectra were measured on a 400 MHz wide bore Varian spectrometer with a triple resonance probe (^{1}H, ^{13}C, ^{15}N), under magic angle spinning. The magic angle was set using KBr, and adamantane was used as reference.

Rehydratation

Fibres from unlabelled amphiphiles were prepared following the standard method with a concentration of 2 mg mL^{-1}, followed by freeze-drying and rehydratation of the sample in a humid environment for 0, 1 and 3 h. ^{13}C spectra were measured using cross-polarisation and under 3.5 kHz magic angle spinning. The 90° pulse on protons was 2.4 μs, the contact time 2.2 ms. Proton decoupling was performed at 75 kHz, using a TPPM sequence, with pulses of 35° with a length of 6.3 μs.

Variation of preparation method

The ^{15}N spectra of 100 % labelled fibres prepared *via* several methods (a–d) were compared. a) PA **1** (2 mg mL^{-1}) was prepared following the standard method and freeze-dried. b) PA **1** (2 mg mL^{-1}) was prepared following the standard method, but omitting the heating step to 90 °C and lyophilised. c) PA **1** (2 mg mL^{-1}) was divided into six fractions which were ultra-centrifuged at 50 rpm, applying a force of 302 g. The pellets were combined and lyophilised. d) PA **1** was prepared at a concentration of 2 mg mL^{-1} using the standard method but using buffers with a concentration of 0.2 M instead of milli Q water as solvent (pH 4: ammonium acetate–acetic acid; pH 7: ammonium carbonate–acetic acid; pH 10: ammonium carbonate–ammonia). Nitrogen spectra were measured after lyophilisation.

^{15}N spectra were obtained in a 3.2 mm sample spinner probe, under magic angle spinning of 9 kHz. The 90° pulse on the ^{1}H channel was optimized *via* nutation experiments to be about 2.3 μs (RF field strength 108 kHz). The Hartmann–Hahn condition was set for a contact time of 4 ms between the ^{1}H and ^{15}N, and the RF field strength of ^{1}H was set to 60 kHz. The proton decoupling power and decoupling time were in general about 100 kHz and 5 ms respectively, the decoupling was set using TPPM with an angle of about 17° and a time of about 5 μs. All these parameters were optimised for all experiments. The number of transients was between 11000 and 43000 spectra.

REDOR experiments

For the intramolecular close-contact measurements a solution consisting of 10 % labelled and 90 % unlabelled amphiphile (total concentration 2 mg mL^{-1}) was used to prepare the fibres following the standard method. The measurements were performed with 9 kHz magic angle spinning speed, and the pulse sequence described by Jaroniec *et al.*[23] A cross polarisation time of 2 ms between ^{1}H and ^{15}N

was used. A TPPM proton decoupling was used with an angle of 15° for 6.25 μs. The 180° pulse on ^{13}C was determined to be 12.5 μs (RF strength of 39.9 kHz).

Acknowledgements

For the cryo-TEM measurements we would like to thank Peter Frederik from Maastricht University. For the SAXS measurements in Grenoble we want to thank Kristina Kvashnina and Wim Bras, from BM 26, and Arnold Nijhuis, Martin Feiters and Mark Damen for help with the measurements. We also thank René de Gelder and Carmen Guguta for help with the reflection mode X-ray experiment. For the solid state NMR measurements we would like to thank Ernst van Eck and Jorge Garibay. Peter van Galen is acknowledged for assisting with mass spectrometry. Finally, for the drawing of the 3D models we want to thank Pieter Nieuwland.

References

1 D. W. P. M. Löwik, J. C. M. van Hest, *Self-assembly of Peptide Amphiphiles in Bottom-up Nanofabrication: Supramolecules, Self-Assemblies, and Organized Films*, American Scientific Publishers, Stevenson Ranch, 2009, ch. 54.
2 H. Cui, M. J. Webber and S. I. Stupp, *Pept. Sci.*, 2010, **94**, 1–18.
3 F. Versluis, H. R. Marsden and A. Kros, *Chem. Soc. Rev.*, 2010, **39**, 3434–3444.
4 X. Zhao, F. Pan, H. Xu, M. Yaseen, H. Shan, C. A. E. Hauser, S. Zhang and J. R. Lu, *Chem. Soc. Rev.*, 2010, **39**, 3480–3498.
5 I. W. Hamley, *Soft Matter*, 2011, **7**, 4122–4138.
6 C. Cerami, U. Frevert, P. Sinnis, B. Takacs, P. Clavijo, M. J. Santos and V. Nussenzweig, *Cell*, 1992, **70**, 1021–1033.
7 D. W. P. M. Lowik, I. O. Shklyarevskiy, L. Ruizendaal, P. C. M. Christianen, J. C. Maan and J. C. M. van Hest, *Adv. Mater.*, 2007, **19**, 1191–1195.
8 M. van den Heuvel, D. W. P. M. Lowik and J. C. M. van Hest, *Biomacromolecules*, 2008, **9**, 2727–2734.
9 M. van den Heuvel, H. Baptist, P. Venema, E. van der Linden, D. Lowik and J. C. M. van Hest, *Soft Matter*, 2011, **7**, 9737–9743.
10 D. W. P. M. Lowik, J. Garcia-Hartjes, J. T. Meijer and J. C. M. van Hest, *Langmuir*, 2005, **21**, 524–526.
11 D. W. P. M. Lowik, J. T. Meijer, I. J. Minten, H. van Kalkeren, L. Heckenmuller, I. Schulten, K. Sliepen, P. Smittenaar and J. C. M. van Hest, *J. Pept. Sci.*, 2008, **14**, 127–133.
12 M. van den Heuvel, A. M. Prenen, J. C. Gielen, P. C. M. Christianen, D. J. Broer, D. W. P. M. Lowik and J. C. M. van Hest, *J. Am. Chem. Soc.*, 2009, **131**, 15014–15017.
13 M. van den Heuvel, D. W. P. M. Löwik and J. C. M. van Hest, *Biomacromolecules*, 2010, **11**, 1676–1683.
14 B. E. I. Ramakers, M. van den Heuvel, N. T. I. Spithas, R. P. Brinkhuis, J. C. M. van Hest and D. Lowik, *Langmuir*, 2012, **28**, 2049–2055.
15 A. Ghasparian, K. Moehle, A. Linden and J. A. Robinson, *Chem. Commun.*, 2006, 174–176.
16 D. W. P. M. Löwik, J. Garcia-Hartjes, J. T. Meijer and J. C. M. van Hest, *Langmuir*, 2005, **21**, 524–526.
17 M. Wolffs, S. J. George, Z. Tomovic, S. C. J. Meskers, A. Schenning and E. W. Meijer, *Angew. Chem., Int. Ed.*, 2007, **46**, 8203–8205.
18 M. V. Jagannadham and R. Nagaraj, *J. Pept. Res.*, 2005, **66**, 94–100.
19 Y. Z. Zhang, Y. Paterson and H. Roder, *Protein Sci.*, 1995, **4**, 804–814.
20 X. J. Lu, P. L. Wintrode and W. K. Surewicz, *Proc. Natl. Acad. Sci. U. S. A.*, 2007, **104**, 1510–1515.
21 T. Asakura, H. Sato, F. Moro, Y. Nakazawa and A. Aoki, *J. Am. Chem. Soc.*, 2007, **129**, 5703–5709.
22 R. Tycko, *Q. Rev. Biophys.*, 2006, **39**, 1–55.
23 C. P. Jaroniec, C. E. MacPhee, N. S. Astrof, C. M. Dobson and R. G. Griffin, *Proc. Natl. Acad. Sci. U. S. A.*, 2002, **99**, 16748–16753.
24 M. H. J. Koch, P. Vachette and D. I. Svergun, *Q. Rev. Biophys.*, 2003, **36**, 147–227.
25 M. J. Krysmann, V. Castelletto, A. Kelarakis, I. W. Hamley, R. A. Hule and D. J. Pochan, *Biochemistry*, 2008, **47**, 4597–4605.

26 E. V. Arx, M. Faupel and M. Brugger, *J. Chromatogr., A*, 1976, **120**, 224–228.
27 G. B. Fields and R. L. Noble, *Int. J. Pept. Protein Res.*, 1990, **35**, 161–214.
28 J. W. Van Nispen, J. P. Polderdijk and H. M. Greven, *Recl. Trav. Chim. Pays-Bas*, 1985, **104**, 99–100.
29 E. Kaiser, R. I. Colescot, C. D. Bossinge and P. I. Cook, *Anal. Biochem.*, 1970, **34**, 595–598.
30 I. Horcas, R. Fernandez, J. M. Gomez-Rodriguez, J. Colchero, J. Gomez-Herrero and A. M. Baro, *Rev. Sci. Instrum.*, 2007, **78**, 0137051–0137058.
31 T. C. Huang, H. Toraya, T. N. Blanton and Y. Wu, *J. Appl. Crystallogr.*, 1993, **26**, 180–184.
32 A. J. M. Duisenberg, L. M. J. Kroon-Batenburg and A. M. M. Schreurs, *J. Appl. Crystallogr.*, 2003, **36**, 220–229.